8-16-2022

# Comparative study of tapered versus conventional cylindrical balloon for stent implantation in stenotic tapered artery

Xiang Shen

Jiabao Jiang

Hongfei Zhu

Kaikai Lu

Pengfei Dong

*See next page for additional authors*

## Authors

Xiang Shen, Jiabao Jiang, Hongfei Zhu, Kaikai Lu, Pengfei Dong, and Linxia Gu

HHS Public Access

Author manuscript

*Artif Organs*. Author manuscript; available in PMC 2022 August 16.

Published in final edited form as:

*Artif Organs*. 2020 July ; 44(7): 727–735. doi:10.1111/aor.13661.

# Comparative study of tapered versus conventional cylindrical balloon for stent implantation in stenotic tapered artery

**Xiang Shen**[1], **Jiabao Jiang**[1], **Hongfei Zhu**[1], **Kaikai Lu**[1], **Pengfei Dong**[2], **Linxia Gu**[2]

[1]School of Mechanical Engineering, Jiangsu University, Zhenjiang, China

[2]Department of Mechanical Engineering, University of Nebraska-Lincoln, Lincoln, NE, USA

## Abstract

The natural tapering of coronary arteries often creates a dilemma for optimal balloon sizing during stenting. The influence of different balloon types, namely, a tapered balloon and a conventional cylindrical balloon, on the mechanical performance of the stent as well as arterial mechanics was investigated via the finite element method. Stent free-expansion and stent deployment in a stenotic tapered artery were investigated numerically. The biomechanical behavior of the two balloon types was compared in terms of stent foreshortening, stent deformation, stent stress distribution, and arterial wall stress distribution. Results indicate that balloon types affect the transient behavior of the stent and the arterial mechanics. Specifically, a tapered balloon could maintain the natural tapering of the coronary artery after stent expansion. In contrast to a cylindrical balloon, tapered balloon also mitigated the foreshortening of the stent (7.69%) as well as the stress concentration in the stent and artery (8.61% and 4.17%, respectively). Hence, tapered balloons should be used in tapered arteries as they may result in low risk of artery injury. This study might provide insights for improved balloon choice and presurgical planning.

### Keywords

arterial mechanics; balloon configuration; finite element analysis; stent expansion; tapered artery; tapered balloon

## 1 | INTRODUCTION

Vascular stenting is widely used to treat artery stenosis owing to its high initial success rate and minimally invasive nature.[1] Currently, the majority of coronary stents can be expanded using a balloon. Conventional balloons are cylindrical and have uniform diameters usually. However, the clinician may be faced with a difficult dilemma when stents need to be implanted into a tapered artery,[2,3] which has a diameter discrepancy between the proximal and distal end. On the one hand, stent and balloon selection based on the larger proximal reference diameter may result in over-dilatation of the distal segment, and thus, an increased

**Correspondence** Xiang Shen, School of Mechanical Engineering, Jiangsu University, No. 301 xuefu Road, Zhenjiang 212013, China. sx@ujs.edu.cn.

CONFLICT OF INTEREST

The authors declare that they have no conflict of interests with the contents of this article.

risk of artery injury.[4] On the other hand, stent and balloon sizing based on the smaller distal reference diameter may result in inadequate dilatation of the proximal segment, and thus, increased residual stenosis. To overcome these shortcomings, a compromise method comprising multiple post-dilations with different cylindrical balloon sizes is often used in clinical practice.[5] Despite this phenomenon, a tapered balloon, which has a decremental diameter, is developed for use in arterial segments with marked tapering between the proximal and the distal reference.[6–8] Clinicians dealing with stenting in the tapered artery attempted to expand the stent using the tapered balloon.[9] Such a process can limit stenting to a single step. Given that different balloon strategies lead to varying results, selecting an optimal balloon strategy for a tapered artery is critical.

Owing to the expense and difficulty involved in the evaluation of stent performance, the finite element method (FEM) is widely used to investigate the mechanical properties of stents and their biomechanical effect on the arteries.[10–20] For example, Cui et al[21] adopted FEM to investigate the effect of balloon length and compliance on vascular stent expansion. De Beule et al[22] used FEM to study the effect of balloon folding on the free expansion of a stent. Schiavone et al[23] used FEM to compare the effect of polyurethane balloon and the three-folded balloon on stent deployment in a stenotic cylindrical artery. Martin et al[24] used FEM to study the effect of a folded configuration of the balloon membrane and its attachment to the catheter on the mechanical behavior of stent and the mechanical environment of the coronary artery. Morlacchi et al[25] used polymeric angioplasty balloons to study the simulations of post-stenting procedures in bifurcated coronary arteries. The majority of computational studies are currently limited to the effect of conventional cylindrical balloon length, fold configuration, and compliance on the deployment of a stent in cylindrical or bifurcated arteries. A detailed comparative study between the application of a tapered and a conventional cylindrical balloon for a tapered artery is lacking, especially on the effects of balloon choices on the expansion characteristics of the stent and on the mechanical environment of the tapered artery.

In this study, two finite element models of the balloon were used to determine the effect of two balloon types on the deployment of a coronary stent. The free expansion of the stent and its expansion in a stenotic tapered coronary artery were investigated using (a) conventional cylindrical balloons model, and (b) tapered balloon model. Various stent performance indicators, including stent foreshortening, stent deformation, stent stress, and arterial stress distributions, were evaluated.

## 2 | MATERIALS AND METHODS

In this study, two sets of finite element analyses were performed using ABAQUS v6.13 (Dassault Systèmes, Vélizy-Villacoublay, France). In the first set of analyses, two models of different shapes of balloons were used to investigate the free deployment of coronary stent. The results from these analyses were compared to determine the effect of balloon shape on the free-deployment characteristics of the stent. In the second set of analyses, the two balloon models were used to investigate the deployment of the same coronary stent within a stenotic tapered artery. The results from these analyses were compared to determine the

influence of balloon shape on the distribution and magnitude of arterial stress induced by a stent.

### 2.1 | Geometry and finite element discretization

The stent investigated resembles the balloon-expandable Palmaz-Schatz coronary stent, as shown in Figure 1. The stent was modeled in Pro/Engineering and then imported into ABAQUS for preprocessing and analysis. In its cylindrical configuration, the stent has an internal diameter of 1.58 mM and a uniform strut thickness of 0.09 mM. The stent had a length of 19.24 mM. The finite element model for free-deployment analysis includes a stent and a tapered balloon or two cylindrical balloons. The finite element model for artery-deployment analysis includes a tapered artery, a plaque, a stent, and a tapered balloon or two cylindrical balloons.

The atherosclerotic coronary artery, which is shown in Figure 2, was a tapered vessel that featured an atherosclerotic plaque at its midsection. The tapered artery was modeled by reducing the external and lumen diameter of the artery linearly along its axis. It had a length of 34 mM. In its tapered configuration, the artery featured a proximal and distal lumen diameter of 3.96 and 2.60 mM, respectively, resulting in a tapered angle of 1.13°. The tapered angle represented the tapering level in the human left coronary artery.[26] The wall thickness of the artery was linearly reduced from the proximal end to the distal end to maintain a constant ratio of wall thickness to the lumen radius ($t/r_i$) as 0.43.[26] The plaque had a length of 17 mM and a maximum thickness of 0.4 mM (middle section). The interfaces between the artery wall and the stenotic plaque were assumed to be a perfect bonding.

The stent was expanded by two balloon types, namely, conventional cylindrical and tapered balloons. The cylindrical balloon with a diameter of 1.5 mM and a length of 21.24 mM was chosen to expand the stent. A second cylindrical balloon was generally used for post-dilatation, especially in the proximal zone of the stent (Figure 1A) to accommodate the tapered artery. The balloon was chosen to have a length and a diameter of 7.1 and 2.2 mM, respectively. The tapered balloon with the same length of 21.24 mM was modeled by a tapered surface with the same taper angle as the artery, leading to a proximal and distal balloon radius of 0.75 and 0.33 mM, respectively.

The balloons were meshed with quadrilateral elements with reduced integration (M3D4R). The stent was meshed with hexahedral elements with reduced integration (C3D8R). The artery mesh was nonuniform with a higher density in the regions of interest. The artery was divided into three regions in the axial direction. Within the end regions, one-way bias was applied with larger elements specified at the ends of the artery, and smaller elements were specified at the outer edges of the central region. The artery and plaque were meshed with C3D8R. A mesh sensitivity study was conducted to ensure the sufficient meshing refinement.

The FEA models of cylindrical and tapered balloons in a tapered artery are shown in Figure 3. All components (ie, stent, artery, and balloon) were coaxial, and the middle points of their axes were overlapping, except the post-dilation cylindrical balloon. The center of the

post-dilation cylindrical balloon was located in plane A of a stent in the axial direction (Figure 1A). Owing to circumferential symmetry, only one-eighth of the circumference of both finite element models was modeled to save computational resources.

## 2.2 | Material properties

The material of the stent is 316L stainless steel, which has elastic-plastic constitutive behavior. The material has a Young's modulus of 201 GPa and a Poisson's ratio of 0.3.[27] The artery is described by the third-order Ogden hyperelastic model. The third-order Ogden hyperelastic strain energy potential is provided by the following equation:

$$W = \sum_{i=1}^{3} \frac{2\mu_i}{\alpha_i^2}\left(\lambda_1^{\alpha_i} + \lambda_2^{\alpha_i} + \lambda_3^{\alpha_i} - 3\right) + \sum_{i=1}^{3} \frac{1}{D_i}(J-1)^{2i} \quad (1)$$

where $\lambda_i (i = 1, 2, 3)$ are the stretches in the three principal directions, and $\mu_i$(MPa) $\alpha_i$ and $D_i$ are model parameters. In this model, $\mu_i$ and $\alpha_i$ are associated with the shear modulus, which can be calculated using the equation, $\mu = \frac{1}{2}\sum_{i=1}^{3} \mu_i \alpha_i$, and $D_i$ represents the compressibility.

In this study, the artery and the plaque are assumed to be nearly incompressible. This assumption was realized by specifying a Poisson's ratio of 0.49 for the material and infinitesimal values for $D_1$ ($D_2 = D_3 = 0$). The same Ogden hyperelastic model was used to describe the constitutive behavior of the hypocellular plaques. The detailed values of the model parameters for the homogeneous artery and plaque[23] are provided in Table 1.

## 2.3 | Boundary and loading

In the cylindrical balloon model, two cylindrical balloons must be used in succession. The first cylindrical balloon (initial balloon) was used to expand the entire stent based on the distal diameter of the artery, and the second cylindrical balloon (post-dilation balloon) was used to post-expand the proximal zone of the stent after the whole stent recoiled based on the proximal diameter of the artery. The entire simulation involved four steps.

Step 1: The first cylindrical balloon experienced radial displacement to deploy the whole stent diameter to 3.234 mM, which is larger by 10% than the lumen diameter of point M in the artery (Figure 2).

Step 2: The stent recoiled with the release of the first cylindrical balloon.

Step 3: The second cylindrical balloon experienced radial displacement to deploy the proximal stent diameter to 3.982 mM, which is larger by 10% than the lumen diameter of point N in the artery (Figure 2).

Step 4: The proximal stent recoiled with the release of the second cylindrical balloon.

Only a tapered balloon is used in the tapered balloon model. The entire simulation involved the following steps:

Step 1: The tapered balloon experienced radial displacement to deploy the stent diameter to 3.234 mM, which is larger by 10% than the lumen diameter of point M in the artery (Figure 2).

Step 2: The stent recoiled with the release of the tapered balloon.

Symmetric constraints were applied to the corresponding symmetric planes. Rotation of all components was inhibited. The artery was constrained in the circumferential direction at points on the symmetry planes, and the ends of the artery were constrained in the axial direction. To prevent the occurrence of stent rigid movement, the middle nodes of the stent in the tapered balloon model were constrained in the axial direction.

### 2.4 | Numerical aspects

The stent was deployed by using cylindrical or tapered balloon with controlled predefined displacement. This method is an optimal choice when simulating stent deployment[22] because the computations are inexpensive. A radial displacement was imposed on the nodes of the cylindrical balloon or tapered balloon to simulate balloon inflation. Inflation and deflation times were 0.1 s. A quasi-static analysis was conducted. The Abaqus/Explicit solver was used for large deformation analyses with the condition that the kinetic energy of the simulation remained below 5% of the total internal energy for each analysis. Surface-to-surface contacts were developed between the outer balloon and the stent inner surface and the stent outer surface and plaque and artery inner surface. All of the contacts were modeled by defining hard normal behavior and a 0.25 frictional coefficient for the tangential contact behavior.[28]

### 2.5 | Post-processing of results

The stent foreshortening, maximum strain, and stress on the stent, artery, and plaque after deployment and recoil were analyzed. The stent foreshortening can be calculated as.

$$\text{Stent foreshortening} = \left(L_{\text{original}} - L\right)/L_{\text{original}} \times 100\% \quad (2)$$

where $L_{\text{original}}$ and $L$ are the original and the final lengths of the stent, respectively.

## 3 | RESULTS

### 3.1 | Free-deployment results

To determine the influence of balloon type on the free-deployment characteristics of the stent, the foreshortening of the stent was measured at final unloading. The foreshortening of the stent was 3.66% and 2.40% for cylindrical and tapered balloons, respectively. The foreshortening observed at the final unloading of the tapered balloon was 34.43% lower than that observed at the final unloading of the cylindrical balloon.

As shown in Figure 4, a distribution of Von Mises (VM) stress was predicted in the stent at maximum loading and final unloading in the free-deployment analyses. For a cylindrical balloon, the maximum expansion refers to the maximum proximal expansion in Step 3. The VM stress distribution in the tapered balloon model is more uniform than that in

the cylindrical balloon model. For the cylindrical balloon model, the maximum stress was distributed in the proximal end of the stent while the stent was in maximum expansion. However, the maximum stress was distributed in the transition region between the central and the proximal end of the stent at the final unloading. For the tapered balloon model, the maximum stress was distributed in the proximal end of the stent at maximum expansion and final unloading of the balloon. The peak stress predicted in the stent at maximum expansion was 521.6 and 509.6 MPa for cylindrical and tapered balloons, respectively. The peak stress predicted in the stent at final unloading was 238.8 and 203.8 MPa for cylindrical and tapered balloons, respectively. Although no significant difference was observed between the peak stress predicted in the stent at maximum expansion, the peak stress predicted in the stent observed at final unloading of the tapered balloon was 14.66% lower than that observed at the final unloading of the cylindrical balloon. Thus, balloon shape greatly affected the stress in the stent.

### 3.2 | Artery-deployment results

With the help of a tapered balloon, the tapered artery maintained the natural taper of the tapered artery during the entire implantation. Figure 5 shows the VM stress distribution in the stented tapered vessel at maximum expansion and final unloading. When the stent was at the maximum expansion, the maximum VM stress was observed near the proximal end of the plaque for the cylindrical balloon model. For the tapered balloon model, the VM stress gradually increased along the distance from proximal to distal, and the maximum VM stress is near the distal end of the plaque. When the stent was at the maximum expansion, the peak stresses predicted in the artery in the cylindrical balloon model (1.24 MPa) was up to 25.81% higher than those in the tapered balloon model (0.92 MPa). When the stent was at the final unloading, the peak stresses predicted in the artery in the cylindrical balloon model (0.24 MPa) were up to 4.17% higher than those observed in the tapered balloon model (0.23 MPa). Given that high stress in arteries is closely related to artery injury and subsequent in-stent restenosis (ISR),[4] a tapered balloon would likely result in a smaller risk of artery injury in comparison with a cylindrical balloon.

As shown in Figure 6, the distribution of VM stress predicted in the plaque is similar to that in the artery at maximum expansion and final unloading. When the stent was at the maximum expansion, the maximum VM stress in the plaque in the tapered balloon model (0.95 MPa) was 27.48% lower than that in the cylindrical model (1.31 MPa). When the stent was at the final unloading, the maximum VM stress in the plaque in the tapered balloon model (0.28 MPa) was 12.50% lower than that in the cylindrical model (0.32 MPa).

At the unloading of balloon models, foreshortening was 2.24% and 2.08% for the cylindrical and tapered balloons, respectively. The foreshortening for the tapered balloon was 7.69% lower than that for the cylindrical balloon. In comparison with the results from the free-deployment analyses, the decrease in rates of foreshortening was attributed to the development of frictional forces between the stent and the artery.

As shown in Figure 7, a distribution of VM stress was predicted in the stent at the maximum expansion diameter and unloading of each of the balloon models. Again, for the cylindrical balloon model, peak stresses were concentrated in the proximal end of stent at the maximum

expansion diameter. However, the peak stress transferred to the transition region between the proximal end and the central part from the proximal stent. For the tapered balloon model, the peak stresses were concentrated in the proximal end in maximum expansion and unloading. The peak stress in the stent at the maximum expansion of tapered balloon (537.00 MPa) was lower by 6.09% than that of the cylindrical balloon (571.80 MPa). The peak stress in the stent at the unloading of the tapered balloon (529.60 MPa) was lower by 8.61% than that of the cylindrical balloon (579.50 MPa).

## 4 | DISCUSSION

The diameter changes of vessels can be encountered because of tapering. This significant diameter change is sometimes the case in carotid artery stenting, but it can also occur in femoral arteries. Although they are rarely examined, coronary arteries also exhibit a degree of taper. Angiographic data suggested that right coronary arteries and left anterior descending taper by approximately 9% and 14%, respectively, along their lengths in men and women.[2] Incomplete stent apposition and vessel wall injury induced by stent expansion are associated with ISR and late stent thrombosis.[29,30] Lumen tapering of the coronary artery can be significant and should be considered in establishing optimal stent implantation criteria to avoid potential complications (ISR and late stent thrombosis). To improve the final apposition of the stent and decrease the risks of stenting failure, an optimal balloon strategy for the tapered artery must be achieved.

Tapered vessels present unique challenges to stent therapy. Although multiple post-dilations with different sizes of conventional balloons were used for tapered vessels, a conventional balloon could not always provide the optimal final appearance. However, a tapered balloon might provide excellent dilation of the stenosis while maintaining the natural taper of the artery. Figure 5 is a clear illustration of segments in which tapered balloons could have achieved an appropriate fit. An optimal fit of the balloon to the dilated segment would provide a more ideal dilation while minimizing injury to the artery. In our study, we focused on the effects of two different balloon shapes on the stent mechanical properties when they were expanded in a stenotic tapered artery. Results showed that a tapered balloon might improve the outcome of stenting in tapered vessels, in contrast to cylindrical balloon. These results seemed consistent with clinical research of Laird et al,[7] in which coronary angioplasty using the tapered balloon catheter appeared to be a safe and effective technique for the treatment of stenotic coronary arteries with marked tapering.

Given that the accuracy of stent implantation in arteries greatly depended on stent foreshortening, a low stent foreshortening rate was expected for a good balloon choice strategy. Besides, low stress in the stent was also expected because great stress in the stent meant that the stent was likely to experience damage. Results confirmed that stent foreshortening rate and VM stress in stents using tapered balloons were lower than those using the cylindrical balloon regardless of stent free-expansion or expansion in the artery. The reason for this result was that the same stent was deployed only once by a tapered balloon and was deployed twice by cylindrical balloons. In addition, when a cylindrical balloon was used to expand a stent in a tapered artery, such post-stenting procedures

might trigger further clinical complications, including artery wall dissection or stent fracture.[27,31,32]

The VM stress was an important indicator of evaluation for stent expansion in vessels because the regions exhibiting the greatest stress in the artery models were also the locations at which most ISRs were reported to occur.[4,33,34] The stress concentration location at the artery and plaque was due to the difference in the expansion method between the cylindrical balloon model and tapered balloon model. Furthermore, the prominent curvature of the plaque geometry at the distal end contributed to stress concentration. Results suggested that different balloon shapes influenced the magnitude and distribution of stress predicted in the artery. The tapered balloon mitigated the stress concentration in the artery, in contrast to the cylindrical balloon. Furthermore, a greater risk of plaque rupture occurred in the cylindrical balloon model than in the tapered balloon model because of the greater stress in the maximum expansion and final unloading (Figure 6). Therefore, the tapered balloon strategy might have lower risk of stenting failure and incidence rate of ISR than the cylindrical balloon strategy.

Our study has several limitations. First, the crimping process of the stent was not considered because crimping had little effect on the mechanical response of the stent and artery after stent expansion. In addition, the artery and plaque were modeled as isotropic materials. A sophisticated material model that considered the collagen fibers of the artery tissue and plaque composition would be preferable. Finally, the artery was modeled with a simplified geometry, whereas a realistic geometry obtained from clinical images could be used. Considering the complexity of realistic vessel model geometry and an anisotropic material model, an idealized stenotic tapered artery model and isotropic material model were adopted for preliminary study. In future research, we will use realistic vessel model geometry and an anisotropic material mode to verify the reliability and universality of conclusions of the article.

## 5 | CONCLUSION

In this study, the influence of two balloon types on the free deployment of the stent and on the mechanical environment of the coronary artery was investigated numerically. The free deployment of the stent and its deployment within a stenotic tapered artery were investigated using (a) a conventional cylindrical balloon model, and (b) a tapered balloon model. Results suggested that balloon type influenced the deformed configuration of the stent and magnitude of stress within the stent and the artery. A tapered balloon model could result in small foreshortening and stress in the stent and artery while maintaining the natural tapering of a tapered artery after effective dilation. Thus, a tapered balloon should be used in tapered arteries. Prior to a stent procedure, this method can be adopted to predict stent apposition and vessel wall stress, thereby selecting the superior stent to be implanted in tapered vessels.

## Funding information

National Natural Science Foundation of China, Grant/Award Number: 51305171; Project of Jiangsu University for training young backbone teachers; Natural Science Foundation of the Higher Education Institutions of Jiangsu

Province, Grant/Award Number: 13KJB460006; Natural Science Foundation of Jiangsu Province, Grant/Award Number: BK20130525; Foundation of Jiangsu University, Grant/Award Number: 10JDG123; China Postdoctoral Science Foundation, Grant/Award Number: 2011M500858

## REFERENCES

1. Ye G, Yin X, Yang X, Wang J, Qi P, Lu J, et al. Efficacy and safety of drug-eluting stent for the intracranial atherosclerotic disease: a systematic review and meta-analysis. J Clin Neurosci. 2019;59:112–8. [PubMed: 30401573]
2. Zubaid M, Buller C, Mancini GB. Normal angiographic tapering of the coronary arteris. Can J Cardiol. 2002;18:973–80. [PubMed: 12368932]
3. Javier SP, Mintz GS, Popma JJ, Pichard AD, Kent KM, Satler LF, et al. Intravascular ultrasound assessment of the magnitude and mechanism of coronary artery and lumen tapering. Am J Cardiol. 1995;75:177–80. [PubMed: 7810498]
4. Timmins LH, Miller MW, Clubb FJ, Moore JE. Increased artery wall stress post-stenting leads to greater intimal thickening. Lab Invest. 2011;91:955–67. [PubMed: 21445059]
5. Tenekecioglu E, Torii R, Bourantas C, Abdelghani M, Cavalcante R, Sotomi Y, et al. Assessment of the hemodynamic characteristics of absorb BVS in a porcine coronary artery model. Int J Cardiol. 2017;227:467–73. [PubMed: 27839816]
6. Banka VS, Baker HA, Vemuri DN, Voci G, Maniet AR. Effectiveness of decremental diameter balloon catheters (tapered balloon). Am J Cardiol. 1992;69:188–93. [PubMed: 1731458]
7. Laird JR, Popma JJ, Knopf WD, Yakubov S, Satler L, White H, et al. Angiographic and procedural outcome after coronary angioplasty in high-risk subsets using a decremental diameter (tapered) balloon catheter. Am J Cardiol. 1996;77:561–8. [PubMed: 8610603]
8. Ragkousis GE, Curzen N, Bressloff NW. Computational modelling of multi-folded balloon delivery system for coronary artery stenting: insights into patient-specific stent malapposition. Ann Biomed Eng. 2015;43:1786–802. [PubMed: 25575740]
9. Zivelonghi C, van Kuijk JP, Nijenhuis V, Poletti E, Suttorp MJ, van derHeyden JAS, et al. First report of the use of long-tapered sirolimus-eluting coronary stent for the treatment of chronic total occlusions with the hybrid algorithm. Catheter Cardio Interv. 2018;92:E299–E307.
10. Imani M, Goudarzi AM, Ganji DD, Aghili AL. The comprehensive finite element model for stenting: the influence of stent design on the outcome after coronary stent placement. J Theor App MechPol. 2013;51:639–48.
11. Ni XY, Pan CW, Prusty BG. Numerical investigations of the mechanical properties of a braided non-vascular stent design using finite element method. Comput Method Biomec. 2015;18:1117–25.
12. Xue Y, Liu X, Sun AQ, Zhang P, Fang YB, Deng XY. Hemodynamic performance of a new punched stent strut: a numerical study. Artif Organs. 2016;40:669–77. [PubMed: 26581476]
13. Shen X, Deng YQ, Ji S, Zhu HF, Jiang JB, Gu LX. Bending analysis of stented coronary artery: the interaction between stent and vessel. J Mech. 2019;35:455–63.
14. Kim DB, Choi H, Joo SM, Kim HK, Shin JH, Hwang MH, et al. A comparative reliability and performance study of different stent designs in terms of mechanical properties: foreshortening, recoil, radial force, and flexibility. Artif Organs. 2013;37:368–79. [PubMed: 23461583]
15. Shen X, Deng Y, Xie Z, Ji S. Assessment of coronary stent deployment in tapered arteries: impact of arterial tapering. J Mech Med Biol. 2016;16:1640015.
16. Chen C, Xiong Y, Jiang W, Wang Y, Wang Z, Chen Y. Experimental and numerical simulation of biodegradable stents with different strut geometries. Cardiovasc Eng Techn. 2020;11:36–46. 10.1007/s13239-019-00433-2.
17. Timmins LH, Meyer CA, Moreno MR, Moore JE. Mechanical modeling of stents deployed in tapered arteries. Ann Biomed Eng. 2008;36:2042–50. [PubMed: 18846425]
18. Schiavone A, Zhao LG, Abdel-Wahab AA. Effects of material, coating, design and plaque composition on stent deployment inside a stenotic artery—finite element simulation. Mater Sci Eng C Mater Biol Appl. 2014;42:479–88. [PubMed: 25063145]

19. Razaghi R, Karimi A, Taheri RA. Patient-specific finite element model of coronary artery stenting. Curr Pharm Design. 2018;24:4492–502.
20. Chen HY, Ai-saadon K, Louvard Y, Kassab GS. Biomechanical impact of provisional stenting and balloon dilatation on coronary bifurcation: clinical implications. J Appl Physiol. 2017; 123:221–6. [PubMed: 28450550]
21. Cui FS, Lee HP, Lu C, Chai P. Effects of balloon length and compliance on vascular stent expansion. Int J Appl Mech. 2010;2:681–97.
22. De Beule M, Mortier P, Carlier SG, Verhegghe B, Van Impe R, Verdonck P. Realistic finiteelement-based stent design: the impact of balloon folding. J Biomech. 2008;41:383–9. [PubMed: 17920068]
23. Schiavone A Computational modelling of stent deployment and mechanical performance inside human atherosclerotic arteries[D]. Leicestershire, UK: © Alessandro Schiavone; 2015.
24. Martin D, Boyle F. Finite element of balloon-expandable coronary stent deployment: influence of angioplasty balloon configuration. Int J Numer Meth Bio. 2013;29:1161–75.
25. Morlacchi S, Colleoni SG, Cárdenes R, Chiastra C, Diez JL, Larrabide I, et al. Patient-specific simulations of stenting procedures in coronary bifurcations: two clinical cases. Med Eng Phys. 2013;35:1272–81. [PubMed: 23428836]
26. Datir P, Lee AY, Lamm SD, Han HC. Effects of geometric variations on the buckling of arteries. Int J Appl Mech. 2011;3:385–406. [PubMed: 22287983]
27. Mehrle A, Skelton T, Almonacid A. Stent fracture: an unusual cause of late restenosis after sirolimus-eluting stent placement. Catheter Cardio Interv. 2007;69:989–92.
28. Ju F, Xia ZH, Sasaki K. On the finite element modelling of balloon-expandable stents. J Mech Behav Biomed. 2008;1:86–95.
29. Buccheri D, Piraino D, Andolina G, Cortese B. Understanding and managing in-stent restenosis: a review of clinical data, from pathogenesis to treatment. J Thorac Dis. 2016;8:E1150–62. [PubMed: 27867580]
30. Attizzani GF, Capodanno D, Ohno Y, Tamburino C. Mechanisms, pathophysiology, and clinical aspects of incomplete stent apposition. J Am Coll Cardiol. 2014;63:1355–67. [PubMed: 24530675]
31. Ye YC, Qian H, Yang M, Zhu X, Gan T, Zhang S, et al. Overexpansion of drug-eluting stents in patients with left main coronary artery disease: an in vivo study. J Int Med Res. 2017;45:1406–16. [PubMed: 28606023]
32. Habib N, van der Heyden J. Acute fracture of ACCULINK carotid stent during post dilation. Catheter Cardio Interv. 2009;74:1107–9.
33. Fujimoto M, Shobayashi Y, Tateshima S, Vinters HV, Vinuela F. Biomechanical responses after Wingspan stent deployment in swine ascending pharyngeal artery. Neurol Res. 2013;35:90–4. [PubMed: 23317803]
34. Fujimoto M, Shobayashi Y, Tateshima S, Vinters HV, Vinuela F. Simulated biomechanical responses at a curved arterial segment after Wingspans stent deployment in swine. Neurol Res. 2013;35:631–5. [PubMed: 23561323]

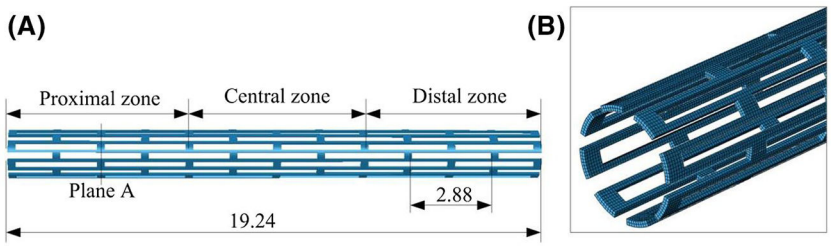


**FIGURE 1.**
Configuration of (A) the stent and (B) the discretized stent

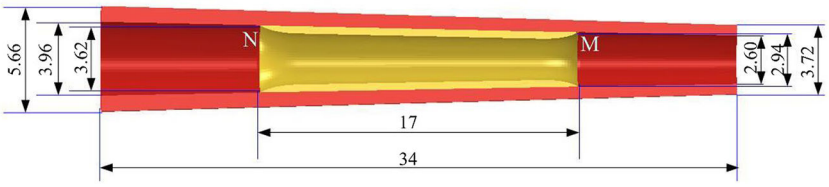


**FIGURE 2.**
Schematic of an atherosclerotic coronary artery with a tapered angle of 1.13°

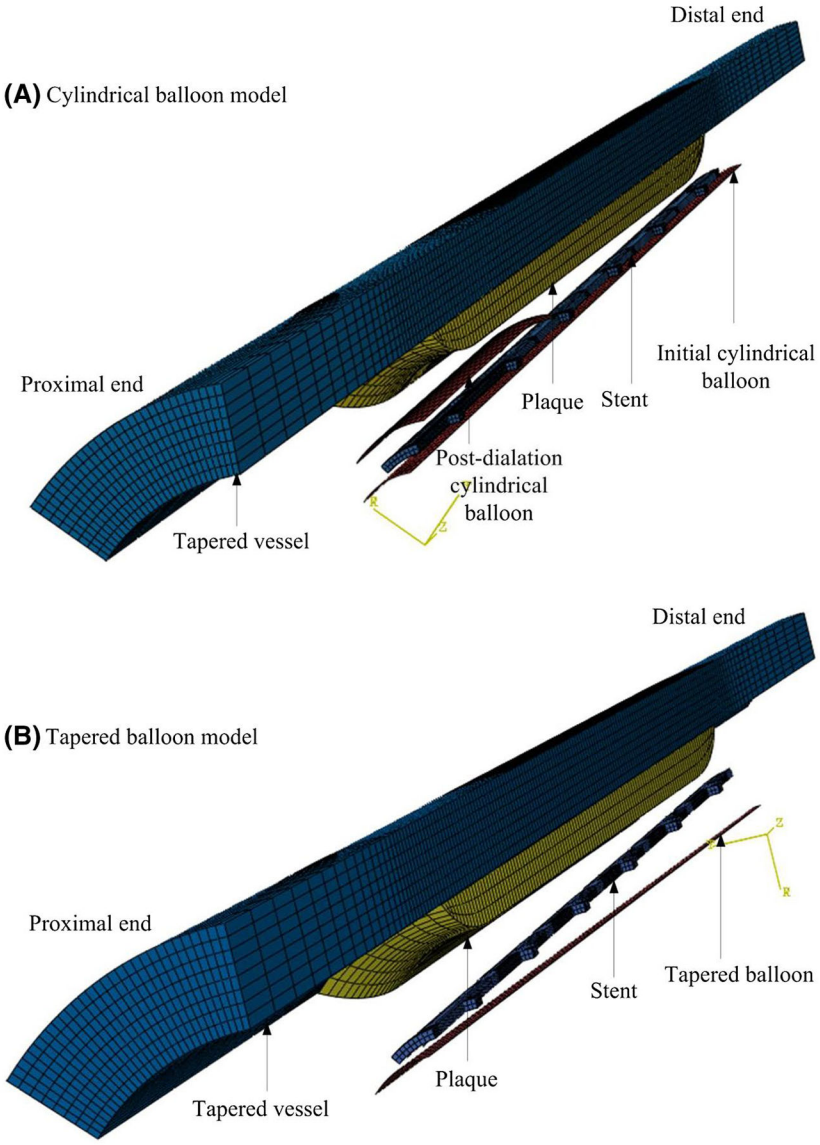


**FIGURE 3.**

Finite element models of stenting tapered artery using (A) cylindrical and (B) tapered balloon

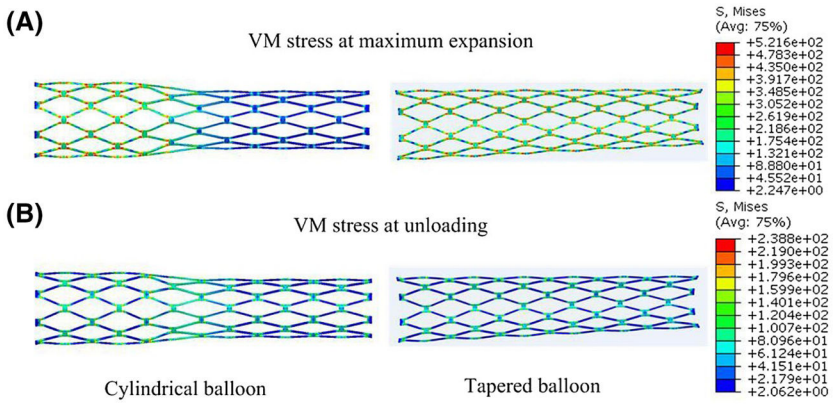


**FIGURE 4.**

VM stress distribution in the stent at (A) maximum expansion (top) and (B) final unloading (bottom) of cylindrical balloon (left) and tapered balloon (right) in the free-deployment analyses

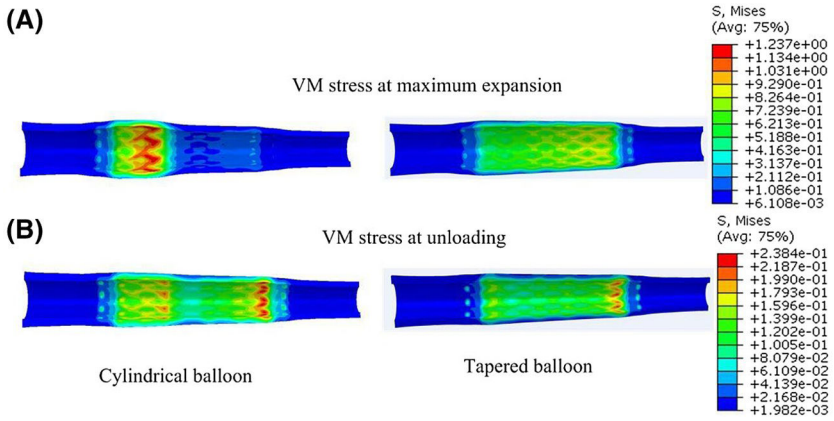


**FIGURE 5.**

VM stress distribution in the artery at (A) maximum expansion (top) and (B) final unloading (bottom) of cylindrical balloon (left) and tapered balloon (right) in the artery-deployment analyses

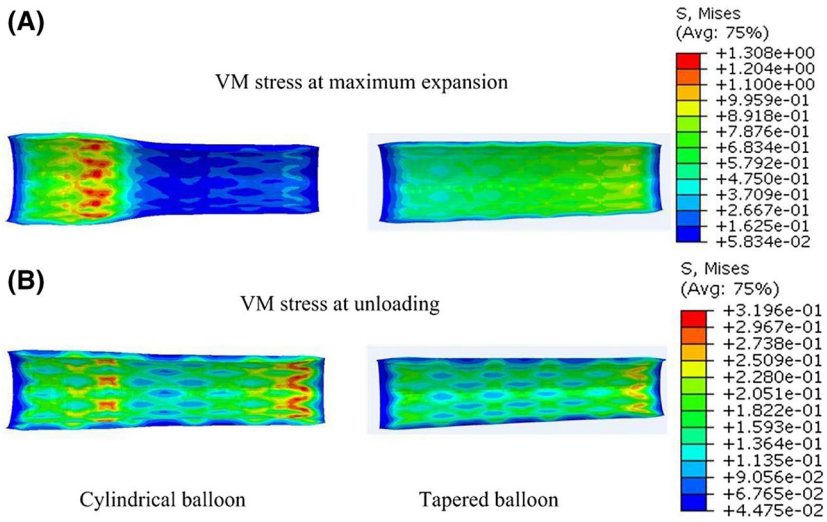


**FIGURE 6.**

VM stress distribution in the plaque at (A) maximum expansion (top) and (B) final unloading (bottom) of cylindrical balloon (left) and tapered balloon (right) in the artery-deployment analyses

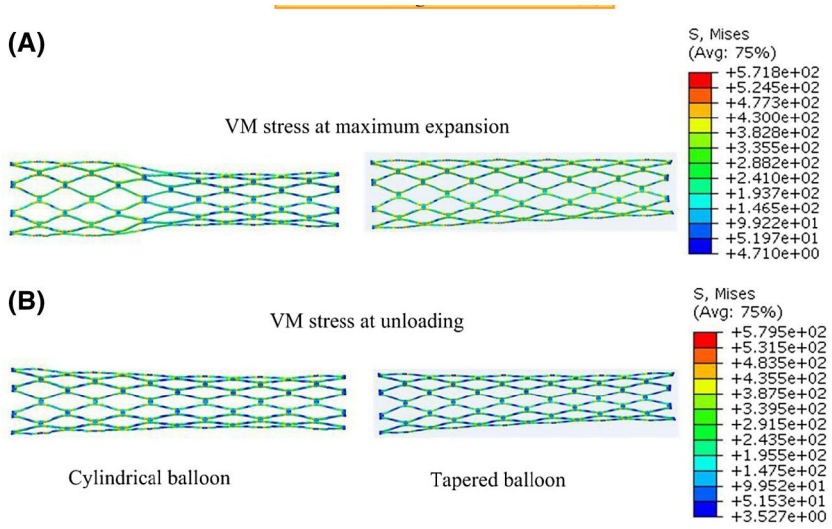


**FIGURE 7.**

VM stress distribution in the stent at (A) maximum expansion (top) and (B) final unloading (bottom) of cylindrical balloon (left) and tapered balloon (right) in the artery-deployment analyses

**TABLE 1**

Hyperelastic material constants used to describe the mechanical behavior of the coronary artery and the atherosclerotic plaque

| Material | $\mu_1$ | $\mu_2$ | $\mu_3$ | $\alpha_1$ | $\alpha_2$ | $\alpha_3$ | $D_1$ | $D_2$ | $D_3$ |
|---|---|---|---|---|---|---|---|---|---|
| Artery | −4.73 | 1.70 | 3.09 | −0.39 | 4.41 | −3.25 | 3.63E-6 | 0 | 0 |
| Plaque | 0.093 | – | – | 8.17 | – | – | 4.30E-7 | – | – |